

Quantum State Transfer in Spin-1 Chains

O. Romero-Isart,¹ K. Eckert,¹ and A. Sanpera^{1,2}

¹*Departament de Física, Grup Física Teòrica, Universitat Autònoma de Barcelona, E-08193 Bellaterra, Spain.*

²*ICREA: Institució Catalana de Recerca i Estudis Avançats.*

(Dated: July 9, 2018)

We study the transfer of quantum information through a Heisenberg spin-1 chain prepared in its ground state. We measure the efficiency of such a quantum channel *via* the fidelity of retrieving an arbitrarily prepared state and *via* the transfer of quantum entanglement. The Heisenberg spin-1 chain has a very rich quantum phase diagram. We show that the phase boundaries are reflected in sharp variations of the transfer efficiency. In the vicinity of the border between the dimer and the ferromagnetic phase (in the conjectured spin-nematic region), we find strong indications for a qualitative change of the excitation spectrum. Moreover, we identify two regions of the phase diagram which give rise to particularly high transfer efficiency; the channel might be non-classical even for chains of arbitrary length, in contrast to spin-1/2 chains.

PACS numbers: 03.67.Hk, 75.10.Jm, 03.75.Mn

Since the early works of Osborne *et al.* [1] and Osterloh *et al.* [2], displaying an intertwined relation between entanglement and quantum phase transitions, the fields of condensed matter and quantum information have developed a strong synergy, further motivated by the spectacular advances reached in the area of ultracold atomic physics and ion traps [3]. Among the broad scope of problems that nowadays can be addressed with ultracold atomic gases, spin models are particularly appealing. These relatively simple models exhibit the most fundamental physics associated with magnetic ordering, criticality, and quantum phase transitions, but mostly lack an analytical solution. Though spin models have been constructed as idealizations or toy models of real systems, ultracold atoms allow for an almost perfect realization of many of them. An example is the one-dimensional (1D) spin-1 system, which can be realized through confining an $S = 1$ spinor condensate in an optical lattice [4, 5]. Restricting to nearest-neighbor interactions, the most general isotropic Hamiltonian for the spin-1 chain is the bilinear-biquadratic Hamiltonian (BBH)

$$\hat{H}(\theta) = J \sum_{\langle ij \rangle} \left[\cos \theta (\vec{S}_i \vec{S}_j) + \sin \theta (\vec{S}_i \vec{S}_j)^2 \right]. \quad (1)$$

Here $\vec{S}_i = (S_i^x, S_i^y, S_i^z)$ are the spin operators on the i th site, and $\cos \theta$ ($\sin \theta$) gives the strength of the bilinear (biquadratic) coupling. The properties of the ground state as well as of the excitations are determined by the angle θ . The phase diagram is shown in Fig. 1(a). In the whole range $-3\pi/4 < \theta < \pi/2$, the ground state is antiferromagnetic, *i.e.*, has vanishing magnetization: $\vec{M} = \langle \sum_i \vec{S}_i \rangle = 0$. Since the Haldane conjecture that 1D isotropic antiferromagnets with integer spin must have a unique massive, *i.e.*, gapped, ground state with exponentially decaying correlations, the BBH has been extensively studied. The Haldane conjecture was rigorously proven for the AKLT point ($\tan \theta = 1/3$), for which Affleck *et al.* explicitly constructed the ground state and proved the existence of a gap [6]. At $\theta = \pi/4$ (Uimin-

Lai-Sutherland point [7, 8]) the system enters into a critical (gapless) phase ($\pi/4 \leq \theta < \pi/2$) with unique ground state and diverging correlation length. At $\theta = -\pi/4$ the gap vanishes [9], but it reopens for $\theta < -\pi/4$, where the system enters into a dimerized phase. The exactly solvable point $\theta = -3\pi/4$ marks the border to the ferromagnetic phase (characterized by $\vec{M} \neq 0$). The existence of a small spin-nematic region between the dimerized phase and $\theta = -3\pi/4$ is actively discussed since a conjecture of Chubukov [10].

In the field of quantum information, spin chains have been intensively studied regarding their usefulness as quantum channels [11, 12, 13]. Attention has been devoted nearly exclusively to spin-1/2 chains, where it has been shown that a general quantum state can be transferred with relatively high fidelity between the two endpoints of a ferromagnetic chain with nearest-neighbor interactions [11, 12]. As models with more complex ground states, spin-1/2 chains in the vicinity of a quantum phase transition [14], spin-1/2 ladders [15] and Peierls distorted chains [16] have been employed as quantum channels.

Here we investigate the usefulness of the spin-1 chain as a quantum channel. To this aim, we study the transmission of an arbitrary quantum state, either pure or

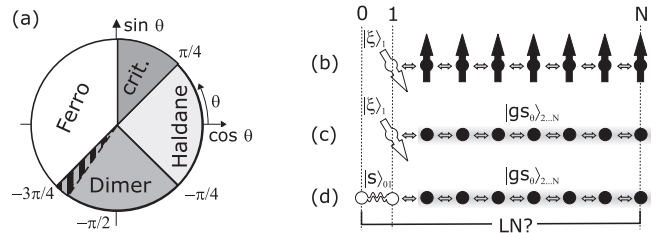


Figure 1: (a) Quantum phases of the spin-1 chain. (b) Scheme for state transfer with an underlying ferromagnetic state, (c) with the channel initialized to the ground state of $\hat{H}(\theta)$, and (d) transfer of quantum entanglement.

entangled with a further subsystem, through the chain prepared in its ground state *for the whole phase diagram*. Compared to previous works studying either the ground state magnetic order or the excitation spectrum of the BBH, our approach combines both aspects simultaneously. We find that the transfer does strongly depend on the nature of the ground state. When crossing the phase boundaries, the quality of the transfer changes sharply. Inside the Haldane phase (around the AKLT point) transfer is very inefficient. On the other hand, high transfer fidelities can be achieved by preparing the spin-1 chain in either the dimerized (gapped) or the critical (gapless) phase. In those cases, transfer fidelities are clearly larger than for a ferromagnetic initial state. Finally, we find a strong reduction of the transfer efficiency for $\theta \gtrsim -3\pi/4$, where a spin-nematic phase has been conjectured. This finding supports recent studies showing a qualitative change in the low-energy excitations as compared to the dimerized phase.

Our scheme for quantum communication generalizes the one usually employed for spin-1/2 systems (Fig. 1(b)): we consider a chain of N sites with the first spin in an arbitrary state $|\xi\rangle_1 = \sum_{m=0,\pm 1} \xi_m |m\rangle_1$ ($S_z|m\rangle = m|m\rangle$, $\sum_m |\xi_m|^2 = 1$) and decoupled from the rest of the chain. The other $N-1$ sites are, for a given θ , prepared in the ground state $|\text{gs}_\theta\rangle_{2\dots N}$ of $\hat{H}(\theta)$. The initial state reads $|\psi_\xi(\theta, t=0)\rangle = |\xi\rangle_1 \otimes |\text{gs}_\theta\rangle_{2\dots N}$, see Fig. 1(c). At $t=0$, we abruptly switch on the interaction between the first and second spin and let the system evolve, obtaining $|\psi_\xi(\theta, t)\rangle = \exp[-it\hat{H}(\theta)]|\psi_\xi(\theta, 0)\rangle$ ($\hbar=1$). At time t , the quality of the transfer of $|\xi\rangle$ to the last spin of the chain is evaluated by the fidelity $\langle \xi | \hat{\rho}_N(\theta, t) | \xi \rangle$ of retrieving $|\xi\rangle$ at the end of the chain. The reduced state of site N is $\hat{\rho}_N(\theta, t) = \text{tr}_{1\dots N-1} |\psi_\xi(\theta, t)\rangle \langle \psi_\xi(\theta, t)|$. The channel fidelity [17] is obtained from averaging over pure states $|\xi\rangle$:

$$F(\theta, t) = \int d\xi \langle \xi | \hat{\rho}_N(\theta, t) | \xi \rangle, \quad (2)$$

where $d\xi$ is the SU(3) invariant measure. For spin-1 always $1/3 \leq F \leq 1$. We define $F(\theta) \equiv F(\theta, t^*)$, where t^* is the time for which the perturbation arrives at the end of the chain for the first time (*i.e.*, we ignore later maxima from multiple reflections on the boundaries).

We also analyze entanglement transfer, considering that the spin at the first lattice site is entangled with a spin outside of the chain, say at lattice site 0 (see Fig. 1(d)). As a particular case we take a singlet state $|s\rangle_{01} = (|1, -1\rangle_{01} - |0, 0\rangle_{01} + |-1, 1\rangle_{01})/\sqrt{3}$, such that initially $|\psi_s(\theta, 0)\rangle = |s\rangle_{01} \otimes |\text{gs}_\theta\rangle_{2\dots N}$. As before, at $t=0$ the coupling between sites 1 and 2 is switched on, while site 0 always remains uncoupled. We quantify the transfer of entanglement to the end of the chain by the logarithmic negativity [18] for sites 0 and N

$$\text{LN}(\theta, t) = \log_2 \|\hat{\rho}_{0N}^\Gamma(\theta, t)\|_1, \quad (3)$$

where $\hat{\rho}_{0N}(\theta, t) = \text{tr}_{1\dots N-1} |\psi_s(\theta, t)\rangle \langle \psi_s(\theta, t)|$, Γ denotes partial transposition, and $\|A\|_1 = \sqrt{\text{tr} A^\dagger A}$. As defined

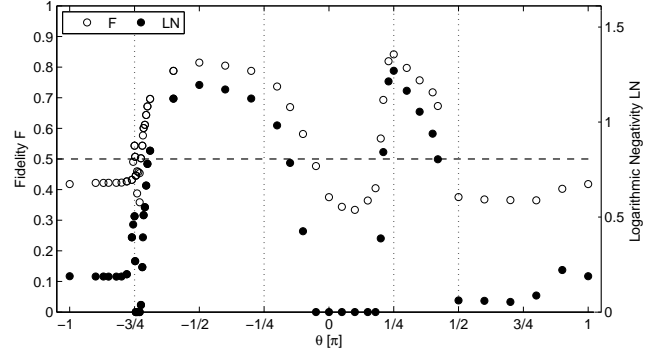


Figure 2: Channel fidelity F (open circles) and entanglement measured *via* logarithmic negativity LN (filled circles) for the transfer between the endpoints of a chain with 25 sites (obtained with MPS methods, using $D = 20 \dots 25$). The dashed horizontal line denotes the maximal fidelity $F_{\text{class}} = 1/2$ which can be obtained through classical communication. Vertical dashed lines indicate the quantum phase boundaries. (See Fig. 4 for a zoom into the region $-0.76\pi \leq \theta \leq -0.7\pi$).

here, $0 \leq \text{LN} \leq \log_2(3)$ gives an upper bound for the number of spin-1/2 singlets that can be distilled from $\hat{\rho}_{0N}(\theta, t)$. Again we will use $\text{LN}(\theta) = \text{LN}(\theta, t^*)$.

We have computed $F(\theta)$ and $\text{LN}(\theta)$ for chains of up to $N = 73$ sites using MPS simulations [19]. Our results for 25 sites and $-\pi \leq \theta < \pi$ are shown in Fig. 2. The different quantum phases of the model are well reflected in the transfer efficiency. Before discussing several interesting points in detail, it is useful to rewrite Eq. (1) in terms of two-site projectors $\hat{P}_{ij}^{(S_T)} = \sum_m |S_T, m\rangle_{ij} \langle S_T, m|$ onto states with total spin S_T ($m = S_T, \dots, -S_T$)

$$\hat{H}(\theta) = J \sum_{\langle ij \rangle} H_{ij}(\theta) = J \sum_{\langle ij \rangle} \lambda_0 \hat{P}_{ij}^{(0)} + \lambda_1 \hat{P}_{ij}^{(1)} + \lambda_2 \hat{P}_{ij}^{(2)}.$$

Here $\lambda_0 = -2 \cos \theta + 4 \sin \theta$, $\lambda_1 = -\cos \theta + \sin \theta$, and $\lambda_2 = \cos \theta + \sin \theta$. We start our discussion at the border of the critical phase and follow the phase diagram in a counter-clockwise order.

(a) *Uimin-Lai-Sutherland point* ($\theta = \pi/4$) and *critical phase* ($\pi/4 < \theta < \pi/2$). Fidelity F and logarithmic negativity LN attain their maximum at $\theta = \pi/4$, and decrease towards the ferromagnetic phase. For $\theta = \pi/4$, the BBH takes a particular simple form

$$\hat{H}_{ij}(\pi/4) = \frac{1}{\sqrt{2}} \left[\vec{S}_i \vec{S}_j + (\vec{S}_i \vec{S}_j)^2 \right] = \frac{1}{\sqrt{2}} \left[\hat{W}_{ij} + \frac{5}{7} \mathbb{1}_{ij} \right], \quad (4)$$

where $\hat{W}_{ij} = (-1)^{2S} \sum_{S_T=0}^{2S} (-1)^{S_T} \hat{P}_{ij}^{(S_T)}$ is the operator swapping sites i and j and $\mathbb{1}_{ij}$ is the identity operator. For $N = 4$, the initial state is $|\psi_\xi(\pi/4, 0)\rangle = |\xi\rangle_1 \otimes |\text{gs}_{\pi/4}\rangle_{234}$, with the trimer state

$$|\text{gs}_{\pi/4}\rangle_{234} = |t\rangle_{234} = \frac{1}{\sqrt{6}} \sum_P (-1)^{|P|} \mathbb{P}_P |1, -1, 0\rangle, \quad (5)$$

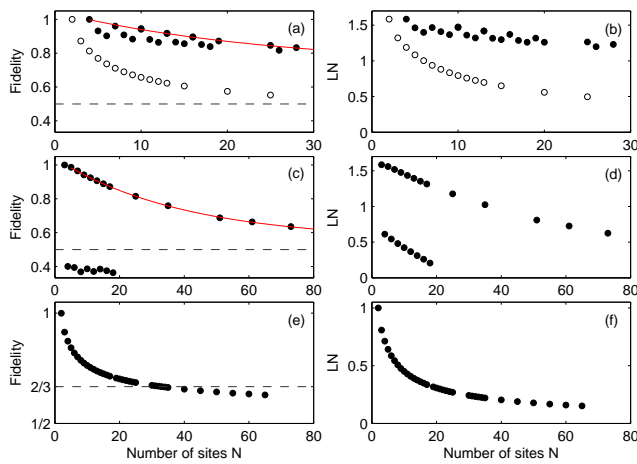


Figure 3: Fidelity F (left column) and logarithmic negativity LN (right column) versus chain length N for (a,b) the spin-1 chain at $\theta = \pi/4$; (c,d) the spin-1 chain at $\theta = -\pi/2$; and (e,f) the spin-1/2 Heisenberg chain. Dark circles correspond to the channel prepared in the ground state, open circles in (a,b) to a ferromagnetic initial state. F is fitted through an exponentially decaying function. Dashed lines indicate the classical communication limit $F_{\text{class}} = 1/2$ ($F_{\text{class}} = 2/3$) for spin-1 (1/2). (Results obtained with MPS simulations using up to $D = 25$ ($D = 24$) for $\theta = \pi/4$ ($-\pi/2$)).

which has total spin zero [20] (P runs over permutations of $\{2, 3, 4\}$, \mathbb{P}_P permutes the sites accordingly). As $|\psi_\xi(\pi/4, Jt = \pi)\rangle = |t\rangle_{123} \otimes |\xi\rangle_4$, perfect transfer ($F = 1$, $\text{LN} = \log_2(3)$) occurs. For $N > 4$, transfer efficiency decreases (dark circles in Fig. 3 (a,b)). For small N the transfer is better for chains of length $N = 1 \bmod 3$, pointing to a trimerized order in the ground state. As N increases this difference vanishes. The average velocity $v = N/t^*$ at which the excitation propagates, grows as N increases. From simulations for $N \leq 28$, we extrapolate $\lim_{N \rightarrow \infty} v \approx 1.59 J \text{ sites}$, a value close to the velocity of sound in the infinite system $v_s = 2\pi/(3\sqrt{2}) J \text{ sites} \approx 1.48 J \text{ sites}$ [8].

To emphasize the role of the initial state of the channel, we use a ferromagnetic state $|\psi_F(t=0)\rangle = |\xi\rangle_1 \otimes |1, 1, \dots, 1\rangle_{2\dots N}$ to compare with. As \hat{H}_{ij} swaps adjacent sites, this reproduces the usual situation for spin-1/2 chains [11, 12]. At time t

$$|\psi_F(\pi/4, t)\rangle = \xi_1 |1 \dots 1\rangle + \sum_{n=1}^N \gamma_{1n}(t) \sum_{i=0, -1} \xi_i |n_i\rangle, \quad (6)$$

where $|n_i\rangle$ represents the state with all spins in state 0, but the n th spin being in $i = 0, -1$. The corresponding probability amplitudes $\gamma_{1n}(t)$ can be calculated as an infinite sum of Bessel functions [21]. Already for $N > 2$, $|\gamma_{1N}(t^*)| < 1$, and thus also $F < 1$. As visible from the open circles in Fig. 3 (a,b), the transfer efficiency for the ferromagnetic initial state is much below the efficiency of

the chain initialized to its ground state.

(b) *Ferromagnetic phase* ($\theta \in (\pi/2, \pi] \cup [-\pi, -3\pi/4)$). This region is characterized by $\lambda_2 < \lambda_0, \lambda_1$. The ground state has ferromagnetic order and broken rotational symmetry: $|\text{gs}_\theta(\vartheta, \varphi)\rangle = \bigotimes_{i=2}^N |1_{\vartheta, \varphi}\rangle_i$. The state $|1_{\vartheta, \varphi}\rangle_i$ has maximal spin projection in the direction specified by (ϑ, φ) . Throughout the whole phase transfer efficiency is very small. The point $\theta = \pi/2$ at the border to the critical phase (where for the finite chain the ground state is ferromagnetic) allows to identify two reasons: (i) for fixed (ϑ, φ) , $|\xi\rangle = |0_{\vartheta, \varphi}\rangle$ having vanishing z -projection in the corresponding direction is not transported; (ii) the transfer of $|\xi\rangle = |-1_{\vartheta, \varphi}\rangle$ is not *via* swaps (as for spin-1/2 or at $\theta = \pi/4$), but through an intermediate state.

(c) *Dimer phase* ($-3\pi/4 < \theta < -\pi/4$). Inside this region, F and LN increase strongly and reach a maximum at $\theta = -\pi/2$. At this point $\lambda_0 < \lambda_1 = \lambda_2$, thus the two-site ground state is a singlet. As $|\xi\rangle_1 \otimes |s\rangle_{23} \pm |s\rangle_{12} \otimes |\xi\rangle_3$ are both eigenstates of $\hat{H}(-\pi/2)$ (with different eigenvalues), for $N = 3$ perfect transfer occurs. For larger (odd) N the ground state of the last $N - 1$ spins is dimerized [5, 24], *i.e.*, the expectation values of $\hat{s}_{i,i+1} = |s\rangle_{i,i+1} \langle s|$ are different on even and odd bonds. This is not the case for even N , and correspondingly transfer fidelities vary strongly between even and odd N , see Fig. 3(c,d). Note that $\hat{H}(-\pi/2) = -\hat{H}(\pi/2)$, *i.e.*, the ground state of one model is the state with highest energy of the other, but fidelities observed in both cases are very different. This observation, which indeed can be made also at other points in the phase diagram, is a clear manifestation of the dependence of the transfer on the underlying magnetic order and the nature of low excitations.

Conjectured spin-nematic phase ($-0.75\pi < \theta \lesssim -0.72\pi$). Near the border to the ferromagnetic phase, Fig. 2 shows a remarkable drop-off in transfer efficiency. Fig. 4(a) shows a zoom into this region where a spin-nematic phase has been suggested [10]. This claim has been actively discussed recently but a complete characterization of this region is still under discussion [5, 22, 23, 24, 25, 26, 27]. The dip for F and LN however is consistent with the results of Läuchli *et al.* [26] and Porrás *et al.* [27], who found a qualitative change in the excitation spectrum for values $-3\pi/4 < \theta < \theta_C$, with $\theta_C/\pi \approx -0.7 \dots -0.67$. To better characterize the ground state in this region, we calculate dimerization, nematic order parameter and magnetization (see Fig. 4(b-d)).

(d) *Haldane phase* ($-\pi/4 < \theta < \pi/4$). A large region in this phase shows poor transfer with fidelities close to the lower limit $F = 1/3$. At the AKLT point ($\tan\theta = 1/3$) this can be understood from the equivalence of the spin-1 chain to a model of two coupled spin-1/2 chains [22]: while the couplings between the two chains are completely symmetric, the AKLT ground state presents an asymmetry due to the boundary spin-1/2s [6]. This may lead to low transfer efficiency.

Let us finally discuss quantitative features by comparing to the spin-1/2 chain without local engineering of couplings [29]. Contrary to Ref. [11], where such a sys-

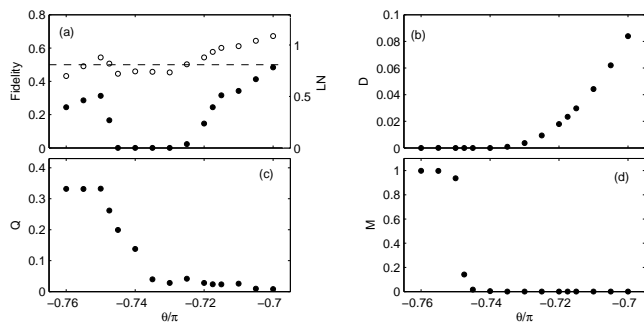


Figure 4: (a) F (open circles) and LN (filled circles) around the region for which a spin-nematic phase has been conjectured (for $N = 25$). The transfer efficiency is strongly reduced for $-0.75\pi < \theta \lesssim 0.72\pi$, as most clearly visible from $\text{LN} = 0$. To characterize the ground state we plot (b) the dimerization $D_{(N-1)/2}$ ($D_i = \langle \hat{H}_{i,i+1} \rangle - \langle \hat{H}_{i+1,i+2} \rangle$), (c) the nematic order parameter $Q = \max_{\Omega} \sum_{i=2}^N [(\vec{n}_{\Omega} \vec{S}_i)^2 - 2/3]/(N-1)$ (\vec{n}_{Ω} is the unit vector pointing in direction Ω), and (d) the magnetization $M = \max_{\Omega} \sum_{i=2}^N \langle \vec{n}_{\Omega} \vec{S}_i \rangle / (N-1)$.

tem was introduced, we always calculate F and LN for the *first* maximum, disregarding better values at (possibly much) later times due to multiple reflections and constructive interference [30]. F and LN for the spin-1/2 chain initialized to a ferromagnetic state and using a Heisenberg Hamiltonian are plotted in Fig. 3 (e,f). A good criterion to evaluate the efficiency of the channel is to compare its fidelity with the highest fidelity for transmission of a quantum state through a classical channel $F_{\text{class}} = 2/(d+1)$, being d the dimension of the quantum system [17]. In particular, we can compute the maximal length of the channel, *i.e.*, the maximal number of sites

for which $F > F_{\text{class}}$. According to our numerical results, for the spin-1/2 chain we obtain $F < F_{\text{class}} = 2/3$ for $N \leq 33$. For spin-1 at $\theta = -\pi/2$ we find that $F > F_{\text{class}} = 1/2$ for all our simulations, *i.e.*, for $N \leq 73$. From fitting the fidelity through an exponentially decaying function, we extrapolate $F_{\infty} = \lim_{N \rightarrow \infty} F \approx 0.56$, indicating that the channel is *always* superior to any classical channel (we cannot exclude a different decay for larger chains, though $N = 73$ is well above the dimer coherence length $N_D \approx 20$ [25]). At $\theta = \pi/4$, fidelities are even larger. Considering chains of $N \leq 28$ sites, we find that fidelity decays exponentially with asymptotic limit $F_{\infty} \approx 0.72$ well above the classical value (again we cannot exclude a different decay for larger chains).

Summarizing, we have studied state and entanglement transfer in spin-1 Heisenberg chains. We have shown that the quality of transfer, characterized by the average fidelity and the logarithmic negativity, undergoes sharp changes at the phase boundaries. The critical (gapless) and the dimerized (gapped) phase have high fidelities; from extrapolating our data the channel might even be non-classical for any number of sites. In contrast, transfer efficiency is significantly lower in the ferromagnetic phase, and attains a minimum in the Haldane phase (around the AKLT point) and in a small region at the border between the dimerized and the ferromagnetic phase, where the existence of a spin-nematic order is controversially discussed.

Acknowledgments – We thank J.J. García-Ripoll and J.I. Cirac for support in developing the MPS code, and M.A. Martín-Delgado and R. Muñoz-Tapia for discussions. We acknowledge support from ESF PESC QUDEDIS and MEC under contracts EX2005-0830, AP2005-0595, FIS 2005-01369/014697, and SGR-00185.

-
- [1] T.J. Osborne and M.A. Nielsen, Phys. Rev. A **66**, 032110 (2002).
 - [2] A. Osterloh *et al.*, Nature **416**, 608 (2005).
 - [3] D. Jaksch *et al.*, Phys. Rev. Lett. **81**, 3108 (1998); M. Greiner *et al.*, Nature **415**, 39 (2002); D. Porras and J.I. Cirac, Phys. Rev. Lett. **92**, 207901 (2004).
 - [4] E. Demler and F. Zhou, Phys. Rev. Lett. **88**, 163001 (2002).
 - [5] S.K. Yip, Phys. Rev. Lett. **90**, 250402 (2003).
 - [6] I. Affleck *et al.*, Phys. Rev. Lett. **59**, 799 (1987).
 - [7] G.V. Uimin, JETP Lett. **12**, 225 (1970); C.K. Lai, J. Math. Phys. **15**, 1675 (1974).
 - [8] B. Sutherland, Phys. Rev. B **12**, 3795 (1975).
 - [9] L.A. Takhtajan, Phys. Lett. A **87**, 479 (1982); H.M. Babujian, Phys. Lett. A **90**, 479 (1982).
 - [10] A.V. Chubukov, Phys. Rev. B **43**, 3337 (1991).
 - [11] S. Bose, Phys. Rev. Lett. **91**, 207901 (2003).
 - [12] V. Subrahmanyam, Phys. Rev. A **69**, 034304 (2004).
 - [13] M. Christandl *et al.*, Phys. Rev. Lett. **92**, 187902 (2004).
 - [14] M.J. Hartmann, M.E. Reuter, and M.B. Plenio, New J. Phys. **8**, 94 (2006).
 - [15] Y. Li *et al.*, Phys. Rev. A **71**, 022301 (2005).
 - [16] M.X. Huo, *et al.*, quant-ph/060602.
 - [17] M. Horodecki, P. Horodecki, and R. Horodecki, Phys. Rev. A **60**, 1888 (1999).
 - [18] M.B. Plenio and S. Virmani, Quant. Inf. Comp. **7**, 1 (2007).
 - [19] G. Vidal, Phys. Rev. Lett. **93**, 040502 (2004); J.J. Garcia-Ripoll, New J. Phys. **8**, 305 (2006).
 - [20] Y. Xian, J. Phys. B: Condens. Matter **5**, 7489 (1993).
 - [21] A. Childs, E. Farhi, and S. Gutmann, Quant. Inf. Proc. **1**, 35 (2002); A.J. Bessen, quant-ph/0609128.
 - [22] Ö. Legeza, G. Fáth, and J. Sólyom, Phys. Rev. B **55**, 291 (1997).
 - [23] B.A. Ivanov and A.K. Kolezhuk, Phys. Rev. B **68**, 052401 (2003).
 - [24] M. Rizzi *et al.*, Phys. Rev. Lett. **95**, 240404 (2005).
 - [25] K. Buchta *et al.*, Phys. Rev. B **72**, 054433 (2005).
 - [26] A. Läuchli, G. Schmid, and S. Trebst, cond-mat/0607173.
 - [27] D. Porras, F. Verstraete, and J.I. Cirac, Phys. Rev. B **73**, 014410 (2006).

- [28] K. Eckert, O. Romero-Isart, and A. Sanpera, quant-ph/0702082.
- [29] In spin-1/2 chains, locally engineering the couplings allows for perfect state transfer [13]. In the spin-1 chain, arbitrarily perfect transfer can be realized *via* adiabatic passage [28].
- [30] In Ref. [11], F is maximized over times up to $Jt = 4000$. For $N = 73$, the first maximum is obtained for $Jt^* \approx 22.5$, *i.e.*, more than 2 orders of magnitude earlier.